Reviewer #1

The manuscript is much improved by the changes made. It is concise, logical, and clearly written. Well done! A few minor suggestions and changes:

Title: The title would be more direct as, 'Why is Trichodesmium abundant…'

We have changed as suggested.

Text:

Line 52: Change 'generally' to 'thought to be'

We have changed as suggested. (L51)

Lines 59-61: What is limited? I think a word is missing.

We have revised the sentence as follows. (L58-60)

"As for phosphorus limitation, iron-enhanced nitrogen fixation causes phosphorus depletion, and the nitrogen fixation is consequently limited by phosphorus (Mather et al., 2008)."

Line 65: Change 'condition' to 'nutrient and trace metal concentrations'

We have changed as suggested. (L64-65)

Line 69: Please give the island names, so that it is clearer how this study differs from previous work.

We have added the island names in the revised manuscript. (L69-70)

Line 88-89: Change 'as summer' to 'summer as'

We have changed as suggested. (L91)

Line 183: Change 'is known' to 'is thought'

We have changed as suggested. (L185)

Line 187: Change 'would' to 'could be higher'

We have changed as suggested. (L189)

Line 194: Please give the incubation time for the tests.

In the experiment1, $^{15}N_2$ gas was injected as bubble form, and the bottle was incubated for at least 12 h to reach equilibrium. Meanwhile, in the experiment2, $^{15}N_2$ dissolved water was made, and thus, the bottle was not incubated. We wrote the detail in the Supplementary Material.

Fig. 3: The horizontal axis labels should be below the graphs

We have changed as suggested.

Fig. 6b: Typo in horizontal axis label.

We have rewritten the label in horizontal axis.

SI:
Line 22: The units and Dabundo reference are missing.

We have added the units. (L22) The Dabundo et al's paper was referred at L7.

Line 28: If it is significant, please add the stats/P-value.

We have added the result of statistics at L29.

Fig. S1: Please describe error bars.

The Error bars indicate standard deviations of the mean (n=5). We have added this sentence in the figure legend.

Fig. S2: Please add the region this figure shows.

We have added the region in this figure.

Fig S3: Would this be clearer on a log scale?

We have changed to a log scale as suggested.

Fig. S4: Please label the x-axis.

We have labeled the x-axis.

Fig. S5: Please label or identify area K.

We have labeled area K in the revised figure.

—

Reviewer #2

I think the manuscript reads more clearly now and the authors have done a good job of addressing reviewers' comments. I suggest a few minor edits:

line 19: The genus Trichodesmium is recognized as an abundant (add the word "an")

We have changed as suggested. (L18)

line 43: oligotrophic conditions (add "s")

We have changed as suggested. (L42)

line 557: conditions (add "s") and phosphate at the nanomolar level (add "the")

We have changed the sentence as follows. (L63-67)

"Therefore, the distinct high abundance of *Trichodesmium* in the Kuroshio is probably not explained by nutrient and trace metal concentrations; however, distributions of dissolved iron and phosphate at the nanomolar level have not been well studied in this region (Obata et al., 1997; Shiozaki et al., 2010; Kodama et al., 2011)."

section 3.2: Perhaps the authors could report the "r squared" value for all of the correlations you report, not just the one on lines 837-838.

We have added the r squared values at L295 and 307.

Why ~~does~~ is *Trichodesmium* ~~become~~ abundant in the Kuroshio?

T. Shiozaki[1,2], S. Takeda[1,3], S. Itoh[2], T. Kodama[1,4], X. Liu[1,5], F. Hashihama[6], K. Furuya[1]

[1]{Department of Aquatic Bioscience, Graduate School of Agricultural and Life Sciences, The University of Tokyo, Tokyo, 113-8657, Japan}

[2]{Atmosphere and Ocean Research Institute, The University of Tokyo, Chiba, 277-8564, Japan}

[3]{Faculty of Fisheries, Nagasaki University, Nagasaki, 852-8521, Japan}

[4]{Japan Sea National Fisheries Research Institute, Fisheries Research Agency, Niigata, 951-8121, Japan}

[5]{College of Ocean and Earth Sciences, Xiamen University, Xiamen, 361005, China}

[6]{Department of Ocean Sciences, Tokyo University of Marine Science and Technology, Tokyo, 108-8477, Japan}

Corresponding to: T. Shiozaki (shiozaki@aori.u-tokyo.ac.jp)

Abstract

The genus *Trichodesmium* is recognized as an abundant and major diazotroph in the Kuroshio, but the reason for this remains unclear. The present study investigated the abundance of *Trichodesmium* spp. and nitrogen fixation together with concentrations of dissolved iron and phosphate in the Kuroshio and its marginal seas. We performed the observations near the Miyako Islands, which form part of the Ryukyu Islands, situated along the Kuroshio, since our satellite analysis suggested that material transport could occur from the islands to the Kuroshio. *Trichodesmium* spp. bloomed (>20,000 filaments L^{-1}) near the Miyako Islands, abundance was high in the Kuroshio and the Kuroshio bifurcation region of the East China Sea, but was low in the Philippine Sea. The abundance of *Trichodesmium* spp. was significantly correlated with the total nitrogen fixation activity. The surface concentrations of dissolved iron (0.19–0.89 nM) and phosphate (<3–36 nM) were similar for all of the study areas, indicating that the nutrient distribution could not explain the spatial differences in *Trichodesmium* spp. abundance and nitrogen fixation. Numerical particle-tracking experiments simulated the transportation of water around the Ryukyu Islands to the Kuroshio. Our results indicate that *Trichodesmium* growing around the Ryukyu Islands could be advected into the Kuroshio.

1. Introduction

The Kuroshio is a western boundary current in the North Pacific Ocean that originates in the North Equatorial Current and bifurcates to the east of the Philippines. The main stream of the Kuroshio enters the East China Sea (ECS) northeast of Taiwan, flows out through the Tokara Strait, and runs along the Japanese islands of Shikoku and Honshu. While the Kuroshio and its adjacent waters are characterized by highly oligotrophic conditions, phytoplankton and zooplankton communities in the Kuroshio are distinct compared to those from adjacent waters (McGowan, 1971). McGowan (1971) suggested that some plankton species are delivered by the Kuroshio to the north from the equatorial region.

The abundance of the cyanobacterial genus *Trichodesmium* in the Kuroshio is much higher than that in neighboring seas (Marumo and Asaoka, 1974). Because *Trichodesmium* is a major nitrogen fixer in the Kuroshio, it is believed to be the key genus for understanding the Kuroshio ecosystem (Chen et al., 2008, 2014; Shiozaki et al., 2014a). Nevertheless, the factors controlling the distribution of *Trichodesmium* in this region are poorly understood. Marine nitrogen fixation is ~~generally~~ thought to be regulated by the supply of iron and phosphorus (Mahaffey et al., 2005), and *Trichodesmium* thrives in iron-rich oligotrophic regions (Moore et al., 2009; Shiozaki

et al., 2010, 2014b). A major source of iron in the ocean is atmospheric dust deposition (Jickells et al., 2005; Mahowald et al., 2009). Modeling studies indicate that dust deposition in the western North Pacific decreases exponentially from the continental shelf to the Philippine Sea (Jickells et al., 2005; Mahowald et al., 2009), and hence, deposition is not as high in the Kuroshio as in the adjacent waters. As for phosphorus limitation, iron-enhanced nitrogen fixation causes phosphorus depletion, and the nitrogen fixation is consequently limited by phosphorus (Mather et al., 2008). The phosphate distribution has been examined in this study region using a conventional colorimetric method, and the surface phosphate concentration in the Kuroshio has been reported to be as low as that in the Philippine Sea (Chen, 2008). Therefore, the distinct high abundance of *Trichodesmium* in the Kuroshio is probably not explained by nutrient ~~condition~~and trace metal concentrations; however, distributions of dissolved iron and phosphate at the nanomolar level have not been well studied in this region (Obata et al., 1997; Shiozaki et al., 2010; Kodama et al., 2011).

Nitrogen fixation by *Trichodesmium* has recently also been found to be active around oceanic islands; New Caledonia Island, Efate Island, Fiji Island, Tahiti Island, and Northern Mariana Islands (Shiozaki et al., 2010, 2013, 2014c; Lin et al., 2011).

Furthermore, these studies demonstrated that abundant *Trichodesmium* is delivered by the current to areas that are remote from the islands. Although this phenomenon was noted in the western Pacific warm pool and western South Pacific, it can also occur in and around the Kuroshio and may contribute to the distribution of *Trichodesmium* in this region.

In the present study, we simultaneously determined *Trichodesmium* abundance and bulk water nitrogen fixation together with concentrations of dissolved iron and phosphate at the nanomolar level in the Kuroshio and its marginal seas. In addition, we conducted intensive observations around the Miyako Islands section of the Ryukyu Islands located close to the main stream of the Kuroshio.

2. Materials and Methods

2.1. Oceanographic database

Algal blooms in an oligotrophic region may indicate a nitrogen fixation hotspot (Wilson and Qiu, 2008; Shiozaki et al., 2014c). To identify the locations of intensive algal blooms, we used a dataset of chlorophyll (chl) *a* observed by satellite. According to Wilson and Qiu (2008), an algal bloom in an oligotrophic region can be defined as a chl *a* value >0.15 mg m^{-3} in summer. In the present study, we used 8-day,

moderate-resolution imaging spectroradiometer (MODIS) level 3 chl *a* with 9 km resolution during summer between July 2003 and September 2009. We defined ~~as~~ summer as July through September. The bloom frequency for each pixel was calculated from the ratio of counts in which chl *a* was >0.15 mg m^{-3} to the total counts in which chl *a* was detected.

To examine the current field, geoelectrokinetograph and ship-mounted acoustic Doppler current profiler (ADCP) data from the uppermost layer for the summers between 1953 and 2008 were obtained from the Japan Oceanographic Data Center (http://www.jodc.go.jp). Regridding, removal of anomalous values, and smoothing of the dataset were performed as described by Isobe (2008).

2.2. **Cruise observations**

Experiments were conducted during summer on-board the R/V *Tansei-maru* (KT-06-21, September 9–17, 2006; KT-07-22, September 5–13, 2007; KT-09-17, September 8–13, 2009; KT-10-19, September 4–12, 2010) and the T/V *Nagasaki-maru* (242, July 19–28, 2007) (Fig. 1a, Table S1). The stations during the KT-06-21, KT-07-22, and *Nagasaki-maru* 242 cruises were divided into three areas based on the temperature-salinity diagram (see Fig.2 of Shiozaki et al., 2011): the

ECS, Kuroshio, and Philippine Sea. During the KT-09-17 cruise, we conducted experiments around the Miyako Islands which were distinguished from the other three areas. During the KT-10-19 cruise, we performed observations in the ECS, the Kuroshio, and around the Miyako Islands (Liu et al., 2013).

2.2.1. **Light intensity, hydrography, nutrients, and chl *a***

Water samples for all of the experiments, with the exception of determination of the dissolved iron concentration, were collected using an acid-cleaned bucket and Niskin-X bottles. The depth profile of light intensity was determined immediately before the water sampling using a light sensor (during the KT-06-22, KT-07-21, KT-09-17, and KT-10-19 cruises) or an empirical equation (during the *Nagasaki-maru* 242 cruise) (Shiozaki et al., 2011). Temperature and salinity profiles to a depth of 200 m were obtained using a conductivity, temperature, and depth (CTD) sensor. Mixed layer depth (MLD) was defined as the depth at which the sigma-t increased by 0.125 from its value at a depth of 10 m. Water samples for nitrate+nitrite (N+N) and phosphate were collected from 0, 10, 30, 40, 50, 60, 70, 80, 90, 100, 125, 150, and 200 m, and from depths at given light intensities. At all of the stations, the N+N and phosphate concentrations were determined at the nanomolar level using a

supersensitive colorimetric system consisting of an AutoAnalyzer II (Technicon) and Liquid Waveguide Capillary Cells (World Precision Instruments, USA) (Hashihama et al., 2009). The detection limits of N+N and phosphate were both 3 nM. When the concentration was greater than 0.1 μM, it was determined by conventional methods using a TRAACS 2000 autoanalyzer (Bran:Luebbe, UK). In addition to the observations at the stations, temperature, salinity, and the *in vivo* chl fluorescence of the surface water were monitored continuously during the cruises by a thermosalinograph (Ocean Seven, Idronaut, Italy) and a fluorometer (Minitracka, Chelsea, UK).

2.2.2. **Dissolved iron**

Water was sampled to estimate the dissolved iron concentration from 0.5-m depth during the KT-06-21 and KT-07-22 cruises and from 10-m depth during the KT-09-17 cruise using an acid-cleaned Teflon bellows pump (AstiPure PFD2; Saint-Gobain) with Teflon tubing (inner diameter = 12 mm). The water was filtered through an acid-cleaned 0.22 μm pore filter (Millipak100; Millipore) connected to the in-line of the Teflon tubing with a Teflon connector. Filtered seawater was collected in a 125 mL low-density polyethylene (LDPE) bottle (Nalgene, Nalge Nunc International),

which had been washed using following technique: the sample bottles were sequentially cleaned by soaking in 5% alkali detergent for at least 2 days, in 4 N HCl for at least 1 day, in 0.3 N metal analysis-grade HNO_3 at 60°C overnight, and finally, in Milli-Q water at 60°C overnight. After rinsing with Milli-Q water, the bottles were dried in a laminar flow space and stored in double plastic bags. The filtrate samples were acidified to a pH <1.7 with trace-metal-grade HCl (Tamapure AA-100; Tama Chemicals) in a Class-100 clean-air bench, and stored at room temperature for more than 1 year.

The dissolved iron concentration was determined using an automatic Fe(III) flow injection analytical system (Kimoto Electric Co., Ltd.) using a chelating resin pre-concentration and chemiluminescence detection method (Obata et al., 1993). A buffer solution of 10 M formic acid and 2.4 M ammonium formate was added to the samples. The sample pH was adjusted to 3.0 with 20% ammonium hydroxide (NH_4OH; Tamapure AA-10; Tama Chemicals) immediately prior to analysis. The detection limit of this method was 0.05 nM. The SAFe reference standards S1 and D2 were measured during the course of sample analysis, and the results were within the range of the published consensus values: S1 = 0.097 ± 0.043 nM and D2 = 0.91 ± 0.17 nM (Johnson et al., 2007).

2.2.3. **Nitrogen fixation and abundance of *Trichodesmium* spp.**

Samples for the incubation experiments were collected vertically at all of the stations, except at Sts. T0621, GN-3, and T0905, where samples were only collected from the surface. All samples were collected in duplicate in acid-cleaned 4.5-L polycarbonate bottles. During the *Nagasaki-maru* 242 cruise, water samples were collected from four different depths corresponding to 100%, 25%, 10%, and 1% of the surface light intensity. During the other cruises, samples were collected from a depth of 50% surface light intensity. Samples at 100% surface light intensity were collected from 0 m during all of the cruises, except during the KT-10-19 cruise in which the samples were collected from a depth of 5 m. The bulk water nitrogen fixation activity was determined based on primary production using a dual isotopic ($^{15}N_2$ and ^{13}C) technique (Shiozaki et al., 2009). After ^{13}C-labeled sodium bicarbonate (99 atom% ^{13}C; Cambridge Isotope Laboratories) was added to each bottle, 2 mL of $^{15}N_2$ gas (98 + atom% ^{15}N; SI Science Co. Japan) was injected directly into the incubation bottles through a septum using a gastight syringe. The bottles were covered with neutral-density screens to adjust the light level and incubated for 24 h in an on-deck incubator cooled by flowing surface seawater for 24 h. We determined the nitrogen

fixation activity using the $^{15}N_2$ gas bubble addition method (Montoya et al., 1996). This method is believed to underestimate the nitrogen fixation rate relative to the $^{15}N_2$ gas dissolution method (Mohr et al., 2010). The start time of incubation in this study varied at each station (Table S1). Considering daily periodicity of nitrogen fixation in each diazotroph (Zehr, 2011) and the time to reach equilibration of the $^{15}N_2$ gas bubble with seawater (>12 h, Mohr et al., 2010), the level of underestimation could vary at each station. Meanwhile, the level of underestimation is ~~known~~ thought to be low in *Trichodesmium* dominant water because *Trichodesmium* can float to the top of the bottle and directly use the added $^{15}N_2$ in the bubble method (Großkopf et al., 2012). Although the bias of underestimation could not be estimated from the results in this study, the actual nitrogen fixation rate ~~would~~ could be higher than the obtained rate.

A recent study demonstrated that commercial $^{15}N_2$ gas could be contaminated by ^{15}N-labeled nitrate and ammonium (Dabundo et al., 2014). We tested the contamination in $^{15}N_2$ gas produced by SI Science Co., Ltd., which was used (from different batch numbers) in the present study (see Supporting Information). Briefly, the $^{15}N_2$ gas was dissolved in aged subtropical surface water, and concentrations of nitrate, nitrite, and ammonium at the nanomolar levels were determined using

199 supersensitive colorimetric systems. The results showed that there were no significant
200 differences between the control and samples to which $^{15}N_2$ had been added (Fig. S1),
201 suggesting that the contamination of nitrate, nitrite, and ammonium in the $^{15}N_2$ gas
202 was insignificant (Supporting Information).

203 Water samples were collected for microscopic analysis at all light depths during
204 the *Nagasaki-maru* 242 and KT-07-21 cruises, and only from the surface during the
205 KT-06-22, KT-09-17, and KT-10-19 cruises. The samples were fixed using acidified
206 Lugol's solution. *Trichodesmium* spp. were counted using the Utermöhl method under
207 inverted microscope observation. *Trichodesmium* greater than ca. 300 μm in length
208 were counted as 1 filament and shorter lengths were counted as 0.5 filaments. In
209 addition, phytoplankton other than *Trichodesmium* spp. were identified from the
210 samples obtained during the KT-09-17 cruise.

211

212 ## 2.3. **Statistical analysis of environmental variables**

213 We used non-metric multi-dimensional scaling (nMDS) to investigate the spatial
214 differences in the environmental variables that could influence *Trichodesmium* growth
215 and bulk water nitrogen fixation; temperature, mixed layer depth, nitrate, dissolved
216 iron, and phosphate. The environmental variables were transformed by $\log_{10}(x + 1)$

prior to analysis. A dissimilarity/similarity matrix between stations was constructed using the Bray-Curtis index. The nMDS was used to visualize similarities in the environmental variables among the stations. An Analysis of Similarity (ANOSIM) was used to test the differences in the environmental variables among the stations.

2.4. **Numerical experiments**

Numerical particle-tracking experiments were conducted to investigate the transport of water masses at the surface from areas around the Miyako Islands in the summer season from 2003 to 2009. Surface velocity data were derived from the FRA-JCOPE2 reanalysis product (Miyazawa et al., 2009), which is an eddy-resolving (1/12°) ocean model combined with three-dimensional variational data assimilation (satellites, ARGO floats, and shipboard observations), and is one of the most reliable models for the region around Japan for the above time period. The method of tracking particles was basically the same as in Itoh et al. (2009), but we did not include the random walk for simplicity. The release points of particles were selected at the surface of the model grid points around the coastal waters of the Miyako Islands. We assumed that the particles did not increase, die, or sink from the surface during the experiments. To focus on transport during the summer season (July–September), particles were

235 released one month before the summer (June 1) and were tracked until September 30.

236 To examine differences in the output depending on the start time within the same
237 year, we also performed experiments starting on June 1, 11, and 21, and July 1 in
238 2009. The ratio of particles that reached areas downstream of the Tokara Strait
239 (hereafter Area K) (Fig. 7), including the particles' entrainment to the Kuroshio, to
240 total particles released from the Miyako Islands was computed in all experiments. It
241 should be noted that these experiments contained the following two uncertainties.
242 First, the distribution of *Trichodesmium* around the islands, which strongly influences
243 the destinations of particles, was not able to be determined in advance.
244 *Trichodesmium* is known to aggregate and not to occur uniformly in the ocean
245 (Capone et al., 1997). Second, the model cannot reproduce the current very close to
246 the islands. If a water mass very near the islands was delivered to the open ocean by
247 tide and/or river plumes that were not considered in the model, seaward dispersion of
248 particles was likely underestimated.

249

250 ## 3. RESULTS

251 ### 3.1. The Kuroshio path and bloom frequency

252 The average surface current field indicated that the main stream of the Kuroshio

253 flowed along the continental shelf in the ECS, and then passed to the south of the
254 Kyushu and Shikoku Islands (Fig. 1b). In addition, the Kuroshio branch bifurcated
255 northward at 25°N and 30°N at the continental shelf. Hence, all of the stations in the
256 ECS were subject to the influence of the Kuroshio. While the northeastward stream of
257 the Kuroshio was prominent in this region, smaller-scale flows and circulations were
258 observed in the areas around and to the southeast of the Ryukyu Islands. In the west of
259 the main stream of the Kuroshio, because the average chl *a* was over 0.15 mg m^{-3} (Fig.
260 S2), the frequency of chl *a* values >0.15 mg m^{-3} was high (Fig. 1b). In contrast, the
261 bloom frequency in the east of the main stream of the Kuroshio differed from the
262 distribution of the average chl *a*; algal blooms occurred frequently in the Ryukyu
263 Islands. Around the Miyako Islands, water of high bloom frequency was located to the
264 west of the islands, extending to the north.
265
266 ### 3.2. Region-wide environmental conditions, *Trichodesmium* spp., and
267 nitrogen fixation
268 The sea surface temperature (SST) ranged from 25.1–30.5°C at all of the stations
269 (Table S1), and there were no significant differences among the areas (p>0.05,
270 Tukey's honestly significant difference [HSD] test). The MLD varied from 12–60 m

271 at all of the stations, and was relatively deep around the Miyako Islands compared to
272 the other areas (Table S1). The surface N+N concentration varied between <3 and 42
273 nM, except around the Miyako Islands (Shiozaki et al., 2010, 2011) (Table S1). The
274 highest surface N+N concentration (374 nM) was observed at St. T0904 where
275 upwelling occurred (see below). No significant difference in the surface N+N was
276 observed among the four areas (p>0.05, Tukey's HSD test). The surface phosphate
277 concentration varied between <3 and 36 nM at all of the stations (Fig. 2a). The
278 phosphate concentration at the surface and within the MLD was not significantly
279 different among the four areas (p>0.05, Tukey's HSD test). There was a greater
280 increase in the phosphate concentrations below 40–50 m in the ECS compared to the
281 other areas (Fig. 3a–d). Furthermore, the phosphate concentrations below 40–50 m
282 near the Miyako Islands were higher than those in the Kuroshio and the Philippine
283 Sea, which were depleted down to 100 m, except at St. T1004 located near the
284 continental shelf. The N/P (= N+N/phosphate) ratio at the surface varied from 0.28 to
285 6.40 except at St. T0904 (N/P = 16.3) (Table S1), and no significant differences were
286 observed among the four areas (p > 0.05, Tukey's HSD test). The surface dissolved
287 iron concentration ranged from 0.19 to 0.89 nM at all of the stations (Fig 2b), with no
288 significant spatial differences among the four areas (p>0.05, Tukey's HSD test). The

289 surface dissolved iron concentration at Sts. T0622 and T0907 was elevated to 0.83 nM
290 and 0.89 nM, respectively, with lower salinity water than in the adjacent waters
291 (salinity data are shown in Fig. 4a and Kodama et al., 2011). The nMDS showed that
292 the environmental variables at all stations were the same at the >80% similarity level
293 and were >90 % similar excepting station T0904 (Fig. 5). The ANOSIM indicated no
294 significant differences among the stations ($p > 0.05$).

295 The abundance of *Trichodesmium* spp. was highest at the surface at almost all of
296 the stations during the *Nagasaki-maru* 242 and KT-07-21 cruises (Fig. S3). The
297 surface *Trichodesmium* spp. abundances were positively correlated with the
298 depth-integrated abundances ($r^2 = 0.51$, $p < 0.05$~~, *t* test~~) (Fig. 6a). Thus, the surface
299 abundance was used to discuss the geographical distribution of *Trichodesmium* spp.
300 The *Trichodesmium* spp. abundance at the surface varied widely, and there was no
301 significant difference among the four areas ($p > 0.05$, Tukey's HSD test).
302 *Trichodesmium* spp. were observed at all of the stations in the Kuroshio and around
303 the Miyako Islands, whereas they were not always observed in the ECS and the
304 Philippine Sea (Fig. 2c). The average surface abundance in the Philippine Sea was the
305 lowest among all of the areas (Table 1). The highest abundance of *Trichodesmium* spp.
306 (>20000 filaments L^{-1}) was observed near the Miyako Islands at St. T0906, where

they bloomed (see below). Tuft-shaped colonies were found at Sts. T0706, T0723, CK-10, and T0906. The nitrogen fixation rate was highest in the upper 25% light depth, and decreased with increasing depth at all of the stations (Fig. 3e–h). The surface rates were positively correlated with the depth-integrated rates ($r^2 = 0.79$, $p < 0.05$~~, *t* test~~) (Fig. 6b), suggesting that the distribution of nitrogen fixation was indexed by the surface activity. Surface and depth-integrated nitrogen fixation ranged from 0.54 to 62 nmol N L^{-1} d^{-1} and from 29.5 to 753 μmol N m^{-2} d^{-1}, respectively (Fig. 2d and Table S1). Surface nitrogen fixation in the Philippine Sea was significantly lower than that in the Kuroshio ($p < 0.05$, *t*-test).

The surface abundance of *Trichodesmium* spp. in the entire study area was positively correlated with the nitrogen fixation rate at the surface ($r^2 = 0.80$; $p < 0.05$ [$r^2 = 0.52$~~5~~; $p < 0.05$ if the datum taken at the *Trichodesmium*-bloom station T0906 is excluded]) (Fig. 6c), suggesting that they significantly contributed to nitrogen fixation in the study region. However, active nitrogen fixation occurred in the ECS where *Trichodesmium* abundance was low, and hence, the other diazotrophs could also be important for nitrogen fixation.

3.3. **Observation around the Miyako Islands during the KT-09-17 cruise**

The SST was lower to the northwest of the Miyako Islands than in adjacent waters, and chl *a* was enriched in the same location (Fig. 4b,c). Therefore, the enhanced productivity was probably due to nutrient supply by upwelling. This upwelling generally occurs in the lee of islands (Hasegawa et al., 2009), suggesting that there was a northward current during the cruise. The surface salinity was lower east of the Miyako Islands than in the surrounding waters (Fig. 4a). The absence of any large river on the east side of Miyako-jima Island and the separation of low salinity water from the island suggest that the low salinity was caused by rainfall.

St. T0904 was located near the upwelling water; its SST of 29.0°C was lowest and its surface N+N concentration of 374 nM was highest among all of the stations. However, the N+N concentration at St. T0904 at the surface was higher than that at the subsurface (an approximate depth of 50 m; Fig. S4), indicating that St. T0904 was not located in the middle of the upwelling. At St. T0904, the surface phosphate concentration was also highest (23 nM) and the N/P ratio (=16.3) was higher than the Redfield ratio. With the exception of the surface at St. T0904, the phosphate concentration was low (<3–9 nM) in the upper 50 m, with no noticeable variation among the stations (Fig. 2a). The dissolved iron concentration varied between 0.19

342 and 0.89 nM at the surface (Fig. 2b). The highest dissolved iron concentration was
343 observed at St. T0907.

344 During the same cruise, we encountered a *Trichodesmium* spp.-bloom at St.
345 T0906 (Fig. 2c), which had colored water at the surface. The abundance of
346 *Trichodesmium* spp. at St. T0906 was >20,000 filaments L^{-1}, which was far higher
347 than that at other stations (2–102 filament L^{-1}). The nitrogen fixation rate at the
348 surface (61.9 nmol N L^{-1} d^{-1}) of this station was more than 30-fold that just below the
349 surface, and was the highest among all of the stations (Fig. 3h). The diatom
350 abundance was markedly higher at St. T0904 than that at the other stations.
351 *Cylindrotheca closterium* was the most numerically dominant diatom (59%), followed
352 by *Navicula* spp. (23%) and *Nitzschia* spp. (13%). *C. closterium* was not detected at
353 the other stations, indicating that the high chl *a* induced by the island wake effect
354 mainly consisted of diatoms.

355

356 ### 3.4. **Numerical simulation**

357 As the Kuroshio generally flows along the continental slope north of the Miyako
358 Islands (Fig. 1b), particles around the Miyako Islands were not transported along the
359 typical path of the Kuroshio to the northeast, especially at their initial stages (Fig. 7a).

Some particles migrated around the Miyako Islands, or turned south after they passed the Tokara Strait. Nevertheless, the particles delivered to Area K east of the Tokara Strait increased as time elapsed, and the ratio of particles delivered to Area K to the total released particles ranged from 13–56% (30 ± 16%) by day 120 in 2003–2009 (Fig. 7b). The year-to-year variations in the ratio are mainly due to influences of mesoscale eddies as partly seen in the particle trajectories in Fig. 7a, and likely occurred over relatively short time scales (shorter than the seasonal time scale). This is supported by another series of experiments in which particles were released on June 1, 11, and 21, and July 1 in 2009, which yielded ratios of 6.2–38% (22 ± 13%) by day 120 (Fig. S5).

4. DISCUSSION

4.1. Distribution of phosphate and dissolved iron concentrations

Phosphate concentrations were consistently low within the MLD in all of the studied areas, and the maximum abundance of *Trichodesmium* spp. and total nitrogen fixation activity generally occurred near the surface, suggesting that the phosphate conditions for surface *Trichodesmium* spp. and other diazotrophs were similar among all of the areas. Furthermore, with the exception of St. T1004 located near the

continental shelf, the vertical distribution of phosphate in the Kuroshio was analogous to that in the Philippine Sea. Therefore, at least in the oceanic region of the two areas, phosphate availability for *Trichodesmium* spp. and the other diazotrophs was similar throughout the water column.

The surface distribution of the dissolved iron concentration demonstrated no significant variation among the areas. The dissolved iron concentration (0.19–0.89 nM) was higher than that in the western North Pacific subtropical region (0.15–0.4 nM) (Brown et al., 2005). Obata et al. (1997) demonstrated that the vertical distribution of the dissolved iron concentration in the ECS showed two peaks (at the surface and in the deep water), suggesting that aerial dust significantly contributes to the high dissolved iron concentration at the surface in all of our study areas. In accordance with our results, previous modeling studies estimated the amount of dust deposition to be similar in all four areas (Jickells et al., 2005; Mahowald et al., 2009). Therefore, iron availability for *Trichodesmium* spp. and the other diazotrophs was also likely similar across all of the study areas. Iron can be supplied from deep water to the surface by mixing processes (Johnson et al., 1999). However, if this were the case, the nitrate concentration would be expected to increase simultaneously at the surface (Johnson et al., 1999), and we observed no noticeable elevation in N+N in any of the

areas, except at St. T0904. High concentrations of dissolved iron (>0.8 nM) corresponded with low salinity at Sts. T0622 and T0907, suggesting that wet deposition was an important process for iron supply. Dry deposition could also be important since the iron-enriched water at Sts. T0601 and T0715 did not correspond with low salinity.

Satellite data analysis indicated that there was a “pipeline” of material transport from the Miyako Islands to the Kuroshio, and this was supported by numerical simulations. According to the hypothesis of Marumo and Asaoka (1974), the growth of *Trichodesmium* in the Kuroshio could be maintained by the supply of iron and phosphorus from the islands situated along the Kuroshio, and the Miyako Islands were considered a possible nutrient source to the Kuroshio. Hence, assuming this hypothesis to be valid, the iron and phosphate concentrations near the Miyako Islands (especially in our observed area) would be expected to be higher than those in the other areas. However, we observed no significant difference in the iron and phosphate concentrations among the four areas. This suggested that there was no detectable washout of iron and phosphorus from the Miyako Islands during our observations, or that diazotrophs and other phytoplankton exhausted the nutrient supply close to the islands.

4.2. Factors controlling the distributions of *Trichodesmium* spp. and nitrogen fixation

Although there was no statistically significant difference in *Trichodesmium* spp. abundance among the study areas probably because the data were limited and the variation was large, *Trichodesmium* spp. were always observed in the Kuroshio and were abundant at most stations. Furthermore, at St.CK-10 in the East China Sea which is in the Kuroshio branch current, a high abundance of *Trichodesmium* spp. was observed. On the other hand, *Trichodesmium* spp. abundance in the Philippine Sea tended to be lower than in the other areas. Such *Trichodesmium* distribution was also reported in the previous study (Marumo and Asaoka, 1974). The present study also showed lower surface nitrogen fixation in the Philippine Sea compared to that in the Kuroshio ($p < 0.05$, *t*-test). Previous studies demonstrated that *Trichodesmium* spp. flourished in some regions of the subtropical ocean where the iron levels were high (Moore et al., 2009; Shiozaki et al., 2014b), which can be attributed to the high iron requirement of *Trichodesmium* spp. for their growth compared to other diazotrophs and non-diazotrophs (Kustka et al., 2003; Saito et al., 2011). Therefore, the distribution of *Trichodesmium* spp. in the study area was expected to be associated

with the dissolved iron concentration at the surface. Furthermore, the iron-enhanced active nitrogen fixation causes phosphorus depletion, and is consequently limited by phosphorus (Mather et al., 2008). No significant differences in surface iron and phosphate were observed among the study areas, which cannot explain the distribution of *Trichodesmium* spp. and nitrogen fixation in the study region.

Johnson et al. (1999) reported that the iron supply increased around the continental shelf because re-suspension from the bottom to the euphotic zone becomes significant. However, in the continental shelf of the ECS, the abundance of *Trichodesmium* spp. and nitrogen fixation were low (Marumo and Asaoka, 1974; Zhang et al., 2012). Zhang et al. (2012) suggested that the low nitrogen fixation in the continental shelf was attributable to mixing processes and the influence of the Changjiang River. Turbulence near the sea floor influences the surface water in the shallower bottom region (Matsuno et al., 2006), and Zhang et al. (2012) suggested that the physical disturbance reduces diazotrophy since diazotrophs including *Trichodesmium* favor calm seas. Furthermore, the water in the continental shelf of the ECS is strongly influenced by the Changjiang River. The N/P ratio of the Changjiang River plume is significantly higher than the Redfield ratio, which results in phosphorus limitation, and can contribute to the low nitrogen fixation (Zhang et al.,

2012). In the present study, despite the fact that the surface phosphate concentration was low throughout the study areas, the N/P ratio was generally lower than the Redfield ratio, suggesting that biological production was limited by the availability of nitrogen compared to phosphate (Moore et al., 2008, 2013). Furthermore, the insignificant difference in MLD among the ECS, the Kuroshio, and the Philippine Sea (p>0.05; Tukey HSD test) indicated similar vertical mixing conditions. Therefore, the environmental variables related to nitrogen fixation only slightly differed as demonstrated by the nMDS plot..

In our study, we found a *Trichodesmium* spp. bloom near the Miyako Islands. Recent studies demonstrated that *Trichodesmium* spp. thrived near oceanic islands (Shiozaki et al., 2010, 2014c; Dupouy et al., 2011). Given that some aspect of the environment around the islands increases *Trichodesmium* spp. abundance and that they are transported from the islands to the Kuroshio, this can explain why the *Trichodesmium* distribution was not estimated from environmental variables. Accordingly, the low abundance of *Trichodesmium* spp. in the Philippine Sea was likely due to the low density of islands. Furthermore, higher nitrogen fixation in the Kuroshio than in the Philippine Sea might be explained in the same manner. *Trichodesmium* is a major nitrogen fixer in the Kuroshio (Chen et al., 2008, 2014;

468 Shiozaki et al., 2014a), and our results showed that the bulk water nitrogen fixation
469 was positively correlated with *Trichodesmium* abundance.

470 The numerical simulation demonstrated that released particles from the Miyako
471 Islands were generally transported to the northeast and flowed along the Kuroshio
472 during summer between 2003 and 2009. Thus, if *Trichodesmium* increases and active
473 nitrogen fixation usually occurs around the Miyako Islands, the water would be
474 delivered to the Kuroshio. Furthermore, we performed additional particle tracking
475 experiments whose particle release points were set at major islands in the Ryukyu
476 Islands (Amami Islands, Okinawa Main Island, and the Ishigaki Islands) (Figs. S6 and
477 S7). The results demonstrated that the particles released from the other islands of the
478 Miyako Islands were also delivered to the Kuroshio, with some exceptions. Based on
479 the calculations for 2003–2009, 13–56% (30 ± 16%) of particles released from the
480 islands reached Area K by day 120 (Fig. S7).

481 Studies on nitrogen fixation around islands in the study region are fairly limited
482 (Liu et al., 2013), and the present study is the first report of a *Trichodesmium* bloom
483 around islands in the area. The Miyako Islands are surrounded by reefs, and studies
484 have shown that *Trichodesmium* blooms can be associated with reef environments
485 (Bell et al., 1999; McKinna et al., 2011). However, the factors causing the

Trichodesmium blooms around islands are not well understood (Shiozaki et al., 2014c). Further studies are required to identify which characteristics of the near island environment are important for the growth and/or accumulation of *Trichodesmium* and other diazotrophs.

5. CONCLUSIONS

We hypothesize that the high abundance of *Trichodesmium* spp. and active nitrogen fixation in the Kuroshio were ascribable not to the unique nutrient environment, but rather to the supply of *Trichodesmium* spp. and other diazotrophs from the surrounding islands. The Ryukyu Islands would not be the only islands with abundant *Trichodesmium* spp., as *Trichodesmium* spp. also flourish in the upstream Kuroshio near Luzon Island (Chen et al., 2008). Therefore, the abundance of *Trichodesmium* spp. would be generally increased around islands situated along the Kuroshio, and the abundant *Trichodesmium* spp. would likely be transported to the mainstream of the Kuroshio. *Trichodesmium* is a major diazotroph in the Kuroshio (Chen et al., 2008, 2014; Shiozaki et al., 2014a), and diazotrophy in the Kuroshio is considered to influence the nutrient stoichiometry in the North Pacific (Shiozaki et al., 2010). Thus, our results indicate that phenomena around the islands located along the

Kuroshio are important for determining the partial nitrogen inventory in the North Pacific.

Author Contributions

T.S., S.T., S.I., and K.F. designed the experiment and T.S., S.T., T.K., X.L., F.H., and K.F. collected the samples at sea. T.S. determined nitrogen fixation and abundance of *Trichodesmium* spp. during the KT-06-21, KT-07-21, KT-09-17, and *Nagasaki-maru* 242 cruises, and X.L. did during the KT-10-19 cruise. T.S. analyzed datasets of satellite and climatological current field. S.T. analyzed concentration of dissolved iron. S.I. performed numerical experiments. T.K. and F.H. determined nutrient concentration. T.S. prepared the manuscript with contributions from all co-authors.

Acknowledgements

We thank J. Ishizaka, the captains, crew members, and participants on board the T/V *Nagasaki-maru* and R/V *Tansei-maru* cruises for their cooperation at sea. Thanks also to K. Hayashizaki for his support in use of the mass spectrometer at Kitasato University, to A. Takeshige and J. Hirai for their valuable comments on biology in the Kuroshio, and to T. Kitahashi for his suggestion on statistical analyses. Comments from two anonymous reviewers greatly improved the paper. We appreciate NASA ocean color processing group for providing the chl *a* data set and Japan Oceanographic Data Center for ADCP data set. This research was financially

525 supported by MEXT grant on Priority Areas (18067006 & 21014006) and by
526 Innovative Areas (24121001, 24121005, & 24121006) and by Grant-in-Aid for JSPS
527 Fellows (25-7341).
528

References

Bell, P.R.F., Elmetri, I., Uwins, P.: Nitrogen fixation by *Trichodesmium* spp. in the central and northern Great Barrier Reef lagoon: relative importance of the fixed-nitrogen load, Mar. Ecol. Progr. Ser., 186, 119-126, 1999.

Brown, M.T., Landing, W.M., Measures, C.I.: Dissolved and particulate Fe in the western and central North Pacific: Results from the 2002 IOC cruise, Geochem. Geophys. Geosyst., 6(10), Q10001, 2005.

Capone, D.G., Zehr, P.J., Paerl, H.W., Bergman, B., Carpenter, E.J.: *Trichodesmium*, a globally significant marine cyanobacterium, Science, 276, 1221-1229, 1997.

Chen, C.T.A.: Distributions of nutrients in the East China Sea and the South China Sea connection, J. Oceanogr., 64, 737-751, 2008.

Chen, Y.L.L., Chen, H.Y., Tuo, S.H., Ohki, K.: Seasonal dynamics of new production from *Trichodesmium* N_2 fixation and nitrate uptake in the upstream Kuroshio and South China Sea basin, Limnol. Oceanogr., 53(5), 1705-1721, 2008.

Chen, Y.L.L., Chen, H.Y., Lin, Y.H., Yong, T.C., Taniuchi, Y., Tuo, S.H.: The relative contributions of unicellular and filamentous diazotrophs to N_2 fixation in the South China Sea and the upstream Kuroshio, Deep-Sea Res. I, 85, 56-71, 2014.

Dabundo, R., Lehmann, M.F., Treibergs, L., Tobias, C.R., Altabet, M.A.: The

547 contamination of commercial $^{15}N_2$ gas stocks with ^{15}N-labeled nitrate and ammonium
548 and consequences for nitrogen fixation measurements, PLoS one, 9(10), e110335,
549 2014.
550 Dupouy, C., Benielli-Gary, D., Neveux, J., Dandonneau, Y., Westberry, T.K.: An
551 algorithm for detecting *Trichodesmium* surface blooms in the South Western Tropical
552 Pacific, Biogeosciences, 8, 3631-3647, 2011.
553 Großkopf, T., Mohr, W., Baustian, T., Schunck, H., Gill, D., Kuypers, M.M.M., Lavik,
554 G., Schmitz, R.A., Wallace, D.W.R., LaRoche, J.: Doubling of marine
555 dinitrogen-fixation rate based on direct measurements, Nature, 488, 361-364, 2012.
556 Hasegawa, D., Lewis, M.R., Gangopadhyay, A.: How islands cause phytoplankton to
557 bloom in their wake, Geophys. Res. Lett., 36, L20605, 2009.
558 Hashihama, F., Furuya, K., Kitajima, S., Takeda, S., Takemura, T., Kanda, J.:
559 Macro-scale exhaustion of surface phosphate by dinitrogen fixation in the western
560 North Pacific, Geophys. Res. Lett., 36, L03610, 2009.
561 Isobe, A.: Recent advances in ocean-circulation research on the Yellow Sea and East
562 China Sea shelves, J. Oceanogr., 64, 569-584, 2008.
563 Itoh, S., Yasuda, I., Nishikawa, H., Sasaki, H., Sasai, Y.: Transport and environmental
564 temperature variability of eggs and larvae of the Japanese anchovy (*Engraulis*

565 *japonicus*) and Japanese sardine (*Sardinops melanostictus*) in the western North
566 Pacific estimated via numerical particle-tracking experiments, Fish. Oceanogr., 18(2),
567 118-133, 2009.Jickells, T.D., An, Z.S., Andersen, K.K., Baker, A.R., Bergametti, G.,
568 Brooks, N., Cao, J.J., Boyd, P.W., Duce, R.A., Hunter, K.A., Kawahata, H., Kubilay,
569 N., LaRoche, J., Liss, P.S., Mahowald, N., Prospero, J.M., Ridgwell, A.J., Tegen, I.,
570 Torres, R.: Global iron connections between desert dust, ocean biogeochemistry, and
571 climate, Science, 308, 67-71, 2005.
572 Johnson, K.S., Chavez, F.P., Friederich, G.E.: Continental-shelf sediment as a
573 primary source of iron for coastal phytoplankton, Nature, 398, 697-700, 1999.
574 Johnson, K.S., Boyle, E., Bruland, K., Coale, K., Measures, C., Moffett, J.,
575 Aguilar-Islas, A., Barbeau, K., Bergquist, B., Bowie, A., Buck, K., Cai, Y., Chase, Z.,
576 Cullen, J., Doi, T., Elrod, V., Fitzwater, S., Gordon, M., King, A., Laan, P.,
577 Laglera-Baquer, L., Landing, W., Lohan, M., Mendez, J., Milne, A., Obata, H.,
578 Ossiander, L., Plant, J., Sarthou, G., Sedwick, P., Smith, G.J., Sohst, B., Tanner, S.,
579 Van den Berg, S., Wu, J.: The SAFe iron intercomparison cruise: an international
580 collaboration to develop dissolved iron in seawater standards, Eos, 88, 131-132, 2007.
581 Kodama, T., Furuya, K., Hashihama, F., Takeda, S., Kanda, J.: Occurrence of
582 rain-origin nitrate patches at the nutrient-depleted surface in the East China Sea and

583 the Philippine Sea during summer, J. Geophys. Res., 116, C08003, 2011.

584 Kustka, A., Sañudo-Wilhelmy, S., Carpenter, E.J., Capone, D.G., Raven, J.A.: A

585 revised estimate of the iron use efficiency of nitrogen fixation, with special reference

586 to the marine cyanobacterium *Trichodesmium* spp. (Cyanophyta), J. Phycol., 39,

587 12-25, 2003.

588 Lin, I.-I., Hu, C., Li, Y.-H., Ho, T.-Y., Fischer, T.P., Wong, G.T.F., Wu, J., Huang,

589 C.-W., Chu, D.A., Ko, D.S., Chen, J.-P. : Fertilization potential of volcanic dust in the

590 low-nutrient low-chlorophyll western North Pacific subtropical gyre: Satellite

591 evidence and laboratory study, Glob. Biogeochem. Cycles, 25, GB1006,

592 doi:10.1029/2009GB003758, 2011.

593 Liu, X., Furuya, K., Shiozaki, T., Masuda, T., Kodama, T., Sato, M., Kaneko, H.,

594 Nagasawa, M., Yasuda, I.: Variability in nitrogen sources for new production in the

595 vicinity of the shelf edge of the East China Sea in summer, Cont. Shelf Res., 61-62,

596 23-30, 2013.

597 McKinna, L.I.W., Furnas, M.J., Ridd, P.V.: A simple, binary classification algorithm

598 for detection of *Trichodesmium* spp. within the Great Barrier Reef using MODIS

599 imagery, Limnol. Oceanogr.; Methods, 9, 50-66, 2011.

600 Mahaffey, C., Michaels, A.F., Capone, D.G.: The conundrum of marine N_2 fixation,

601 Am. J. Sci., 305, 546-595, 2005.

602 Mahowald, N.M., Engelstaedter, S., Luo, C., Sealy, A., Artaxo, P., Benitez-Nelson, C.,

603 Bonnet, S., Chen, Y., Chuang, P.Y., Cohen, D.D., Dulac, F., Herut, B., Johansen,

604 A.M., Kubilay, N., Losno, R., Maenhaut, W., Paytan, A., Prospero, J.M., Shank, L.M.,

605 Siefert, R.L.: Atmospheric iron deposition: Global distribution, variability, and human

606 perturbations, Annu. Rev. Mar. Sci., 1, 245-278, 2009.

607 Marumo, R., Asaoka, O.: *Trichodesmium* in the East China Sea 1. Distribution of

608 *Trichodesmium thiebautii* GOMONT during 1961-1967, J. Oceanogr. Soc. Japan, 30,

609 298-303, 1974.

610 Mather, R.L., Reynolds, S.E., Wolff, G.A., Williams, R.G., Torres-Valdes, S.,

611 Woodward, E.M.S., Landolfi, A., Pan, X., Sanders, R., Achterberg, E.P.: Phosphorus

612 cycling in the North and South Atlantic Ocean subtropical gyres, Nat. Geosci., 1,

613 439-443, 2008.

614 Matsuno, T., Lee, J.S., Shimizu, M., Kim, S.H., Pang, I.C.: Measurements of the

615 turbulent energy dissipation rate ε and an evaluation of the dispersion process of the

616 Changjiang Diluted Water in the East China Sea, J. Geophys. Res., 111, C11S09,

617 2006.

618 McGowan, J.A.: Oceanic biogeography of the Pacific, in: The microplaleontology of

619 the oceans, Cambridge University Press, Cambridge, 3-74, 1971.

620 Miyazawa, Y., Zhang, R., Guo, X., Tamura, H., Ambe, D., Lee, J.S., Okuno, A.,

621 Yoshinari, H., Setou, T., Komatsu, K.: Water mass variability in the western North

622 Pacific detected in a 15-year eddy resolving ocean reanalysis, J. Oceanogr., 65,

623 737-756, 2009.

624 Mohr, W., Großkopf, T., Wallace, D.W.R., LaRoche, J.: Methodological

625 underestimation of oceanic nitrogen fixation rate, PLoS one, 5(9), e12583, 2010.

626 Montoya, J.P., Voss, M., Kähler, P., Capone, D.G.: A simple, high-precision,

627 high-sensitivity tracer assay for N_2 fixation, Appl. Environ. Microbiol., 62(3),

628 986-993, 1996.

629 Moore, C.M., Mills, M.M., Langlois, R., Milne, A., Achterberg, E.P., LaRoche, J.,

630 Geider, R.J.: Relative influence of nitrogen and phosphorus availability on

631 phytoplankton physiology and productivity in the oligotrophic sub-tropical North

632 Atlantic Ocean, Limnol. Oceanogr., 53(1), 291-305, 2008.

633 Moore, C.M., Mills, M.M., Achterberg, E.P., Geider, R.J., LaRoche, J., Lucas, M.I.,

634 McDonagh, E.L., Pan, X., Poulton, A.J., Rijkenberg, M.J.A., Suggett, D.J., Ussher,

635 S.J., Woodward, E.M.S.: Large-scale distribution of Atlantic nitrogen fixation

636 controlled by iron availability, Nat. Geosci., 2, 867-871, 2009.

637 Moore, C.M., Mills, M.M., Arrigo, K.R., Berman-Frank, I., Bopp, L., Boyd, P.W.,
638 Galbraith, E.D., Geider, R.J., Guieu, C., Jaccard, S.L., Jickells, T.D., LaRoche, J.,
639 Lenton, T.M., Mahowald, N.M., Marañon, E., Marinov, I., Moore, J.K., Nakatsuka, T.,
640 Oschlies, A., Saito, M.A., Thingstad, T.F., Tsuda, A., Ulloa, O.: Processes and
641 patterns of oceanic nutrient limitation, Nat. Geosci., 6, 701-710, 2013.
642 Obata, H., Karatani, H., Nakayama, E.: Automated determination of iron in seawater
643 by chelating resin concentration and chemiluminescence detection, Anal. Chem., 65,
644 1524-1528, 1993.
645 Obata, H., Karatani, H., Matsui, M., Nakayama, E.: Fundamental studies for chemical
646 speciation of iron in seawater with an improved analytical method, Mar. Chem., 56,
647 97-106, 1997.
648 Saito, M.A., Bertrand, E.M., Dutkiewicz, S., Bulygin, V.V., Moran, D.M., Monteiro,
649 F.M., Follows, M.J., Valois, F.W., Waterbury, J.B.: Iron conservation by reduction of
650 metalloenzyme inventories in the marine diazotroph *Crocosphaera watsonii*, Proc.
651 Natl. Acad. Sci. USA, 108, 2184-2189, 2011.
652 Shiozaki, T., Furuya, K., Kodama, T., Takeda, S.: Contribution of N_2 fixation to new
653 production in the western North Pacific Ocean along 155ºE, Mar. Ecol. Progr. Ser.,
654 377, 19-32, 2009.

655 Shiozaki, T., Furuya, K., Kodama, T., Kitajima, S., Takeda, S., Takemura, T., Kanda,
656 J.: New estimation of N_2 fixation in the western and central Pacific Ocean and its
657 marginal seas,. Glob. Biogeochem. Cycles, 24, GB1015, 2010.
658 Shiozaki, T., Furuya, K., Kurotori, H., Kodama, T., Takeda, S., Endoh, T., Yoshikawa,
659 Y., Ishizaka, J., Matsuno, T.: Imbalance between vertical nitrate flux and nitrate
660 assimilation on a continental shelf: Implications of nitrification, J. Geophys. Res., 116,
661 C10031, 2011.
662 Shiozaki, T., Chen, Y.L.L., Lin, Y.H., Taniuchi, Y., Sheu, D.S., Furuya, K., Chen,
663 H.Y.: Seasonal variations of unicellular diazotroph groups A and B, and
664 *Trichodesmium* in the northern South China Sea and neighboring upstream Kuroshio
665 Current, Cont. Shelf Res., 80, 20-31, 2014a.
666 Shiozaki, T., Ijichi, M., Kodama, T., Takeda, S., Furuya, K.: Heterotrophic bacteria as
667 major nitrogen fixers in the euphotic zone of the Indian Ocean, Glob. Biogeochem.
668 Cycles, 28, 1096-1110, 2014b.
669 Shiozaki, T., Kodama, T., Furuya, K.: Large-scale impact of the island mass effect
670 through nitrogen fixation in the western South Pacific Ocean, Geophys. Res. Lett., 41,
671 2907-2913, 2014c.
672 Wilson, C., Qiu, X.: Global distribution of summer chlorophyll blooms in the

673 oligotrophic gyres, Progr. Oceanogr., 78, 107-134, 2008.

674 Zhang, R., Chen, M., Cao, J., Ma, Q., Yang, J., Qiu, Y.: Nitrogen fixation in the East

675 China Sea and southern Yellow Sea during summer 2006, Mar. Ecol. Progr. Ser., 447,

676 77-86, 2012.

677

678 Table 1 Summary of *Trichodesmium* at the surface, and depth-integrated nitrogen

679 fixation and its related parameters in the four representative study areas.

Area	*Trichodesmium*[*] [filaments l^{-1}]	N_2 fixation [μmolN L^{-1} d^{-1}]	Temperature[*] [ºC]	MLD [m]	$NO_3^-+NO_2^{-*,\dagger}$ [nM]	$PO_4^{3-*,\dagger}$ [nM]	DFe[*] [nM]
East China Sea	21±58	170±140	28.5±1.2	24±12	19±11	15±9	0.76±0.18
Kuroshio	43±33	199±142	29.4±0.81	27±8	9±8	15±7	0.45±0.13
Philippine Sea	8±8	58.3±25.1	29.4±0.1	23±3	8±3	14±19	0.51±0.25
Miyako Islands	3019±8478	201±274	29.3±0.3	40±12	61±128	8±7	0.38±0.24

680 [*] values in surface water

681 [†]When the concentration was below the detection limit (3 nM), we assumed a concentration of 3 nM to

682 calculate the mean.

683

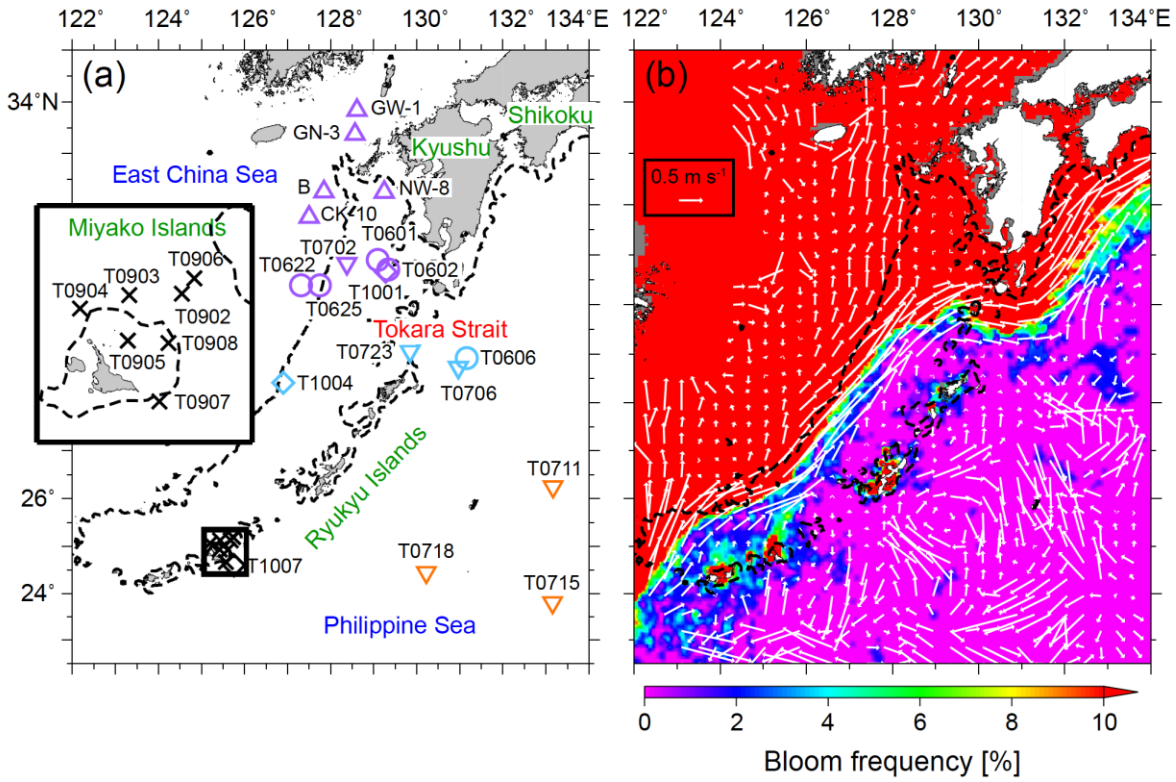

684

685

686 Figure 1. (a) Sampling stations during the KT-06-21 (circles), KT-07-22 (inverted
687 triangles), KT-09-17 (crosses), KT-10-19 (diamonds), and 242 (triangles) cruises.
688 Symbols of stations located in the East China Sea, the Kuroshio, the Philippine Sea,
689 and near the Miyako Islands are indicated in purple, light blue, orange, and black,
690 respectively. (b) Climatological surface current fields during summer (1953–2008)
691 from geoelectrokinetograph measurements and ship-mounted ADCP data. The
692 background contour represents the percentage of chlorophyll *a* of >0.15 mg m^{-3}
693 during summer between 2003 and 2009. Dashed lines indicate 200 m isobaths.

694

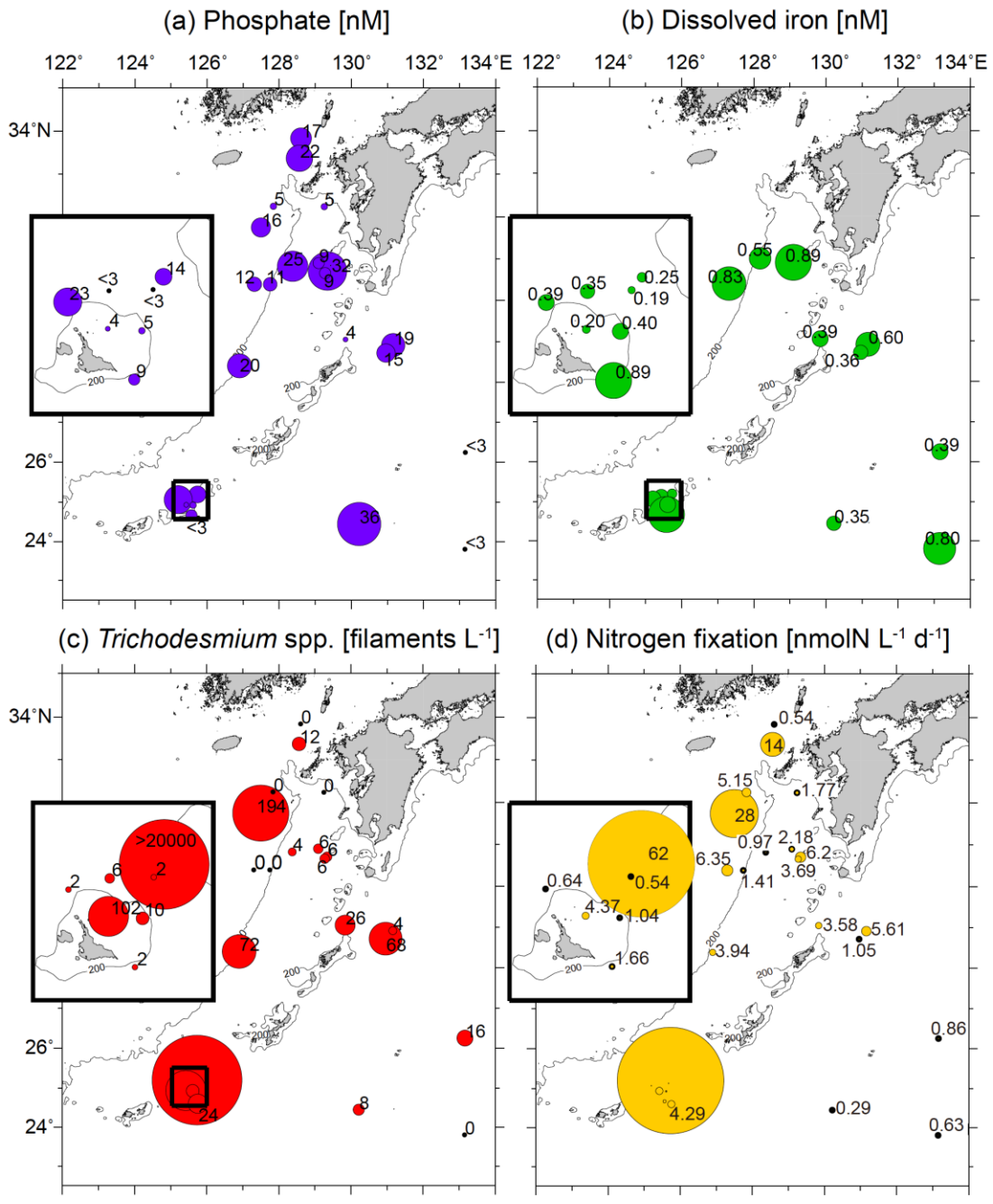

Figure 2. Distribution of (a) phosphate, (b) dissolved iron, (c) *Trichodesmium* spp., and (d) nitrogen fixation at the surface. The parameters in the small boxes indicate results from the KT-09-17 cruise. The areas of the circles are proportional to the concentration, abundance, or activity.

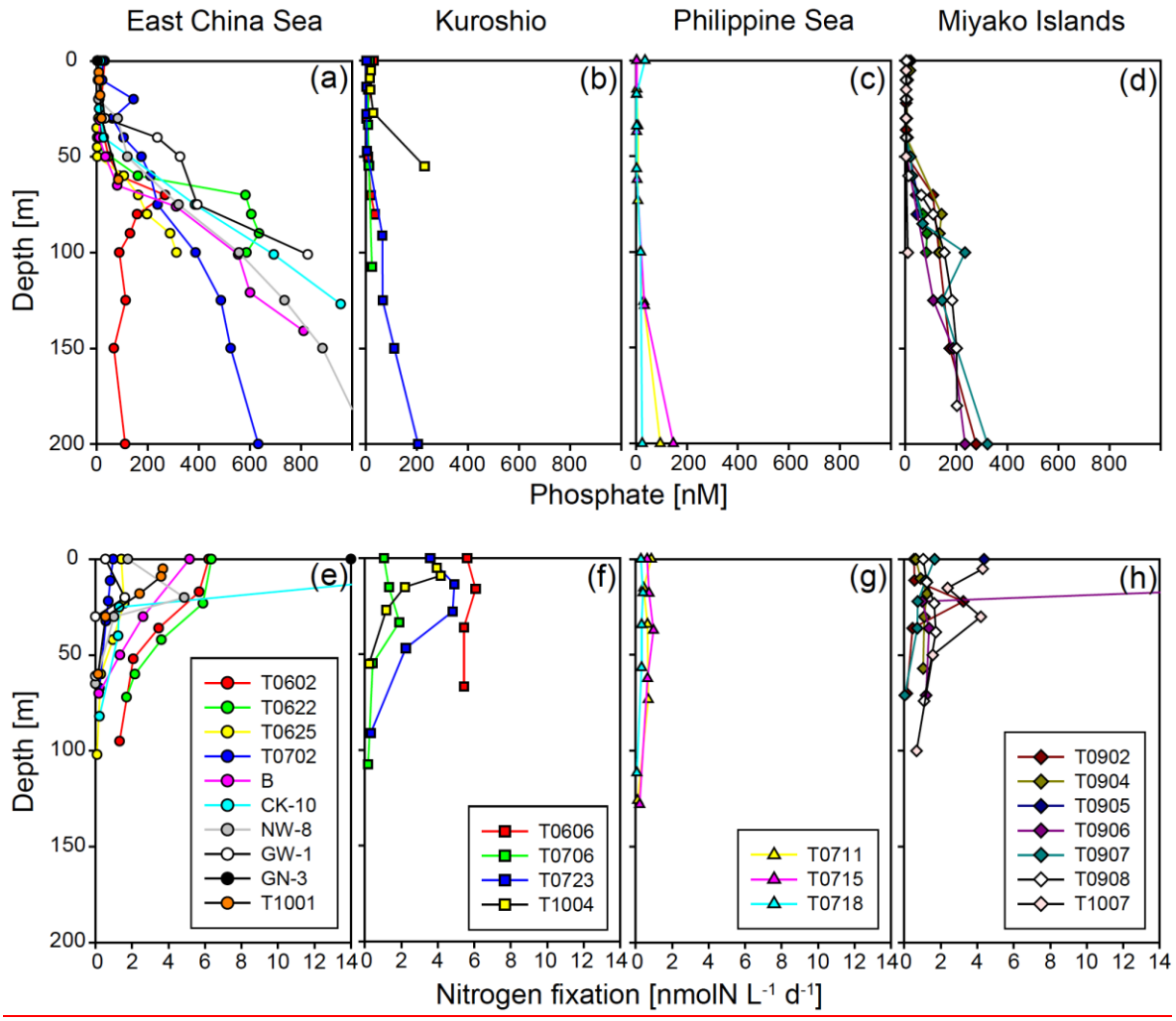
East China Sea
Kuroshio
Philippine Sea
Miyako Islands
(a)
(b)
(c)
(d)
Depth [m]
Phosphate [nM]
(e)
(f)
(g)
(h)
T0602
T0622
T0625
T0702
B
CK-10
NW-8
GW-1
GN-3
T1001
T0606
T0706
T0723
T1004
T0711
T0715
T0718
T0902
T0904
T0905
T0906
T0907
T0908
T1007
Nitrogen fixation [nmolN L-1 d-1]

701

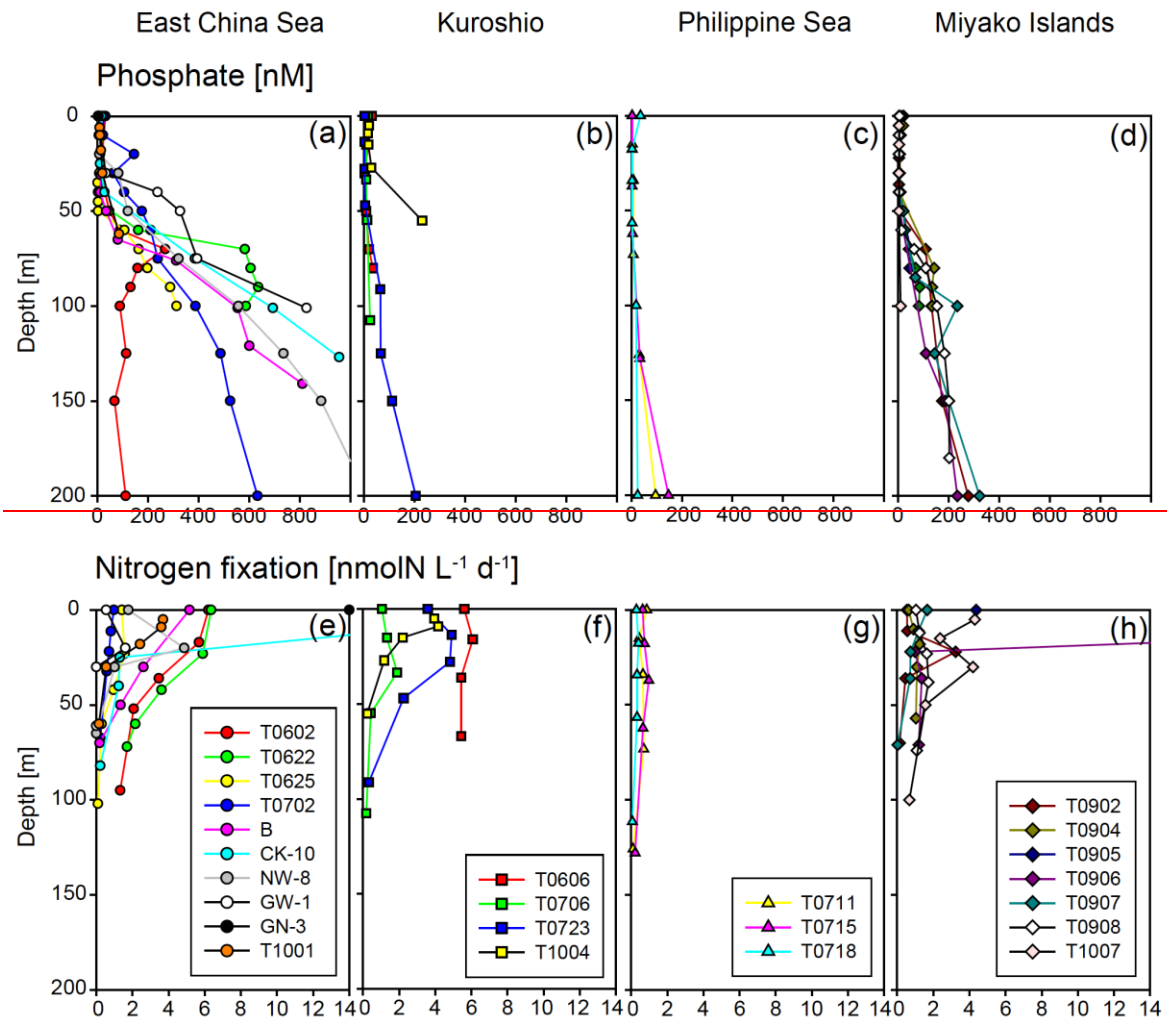

Figure 3. Vertical profiles of phosphate and nitrogen fixation in the East China Sea (a and e), the Kuroshio (b and f), the Philippine Sea (c and g), and the Miyako Islands (d and h).

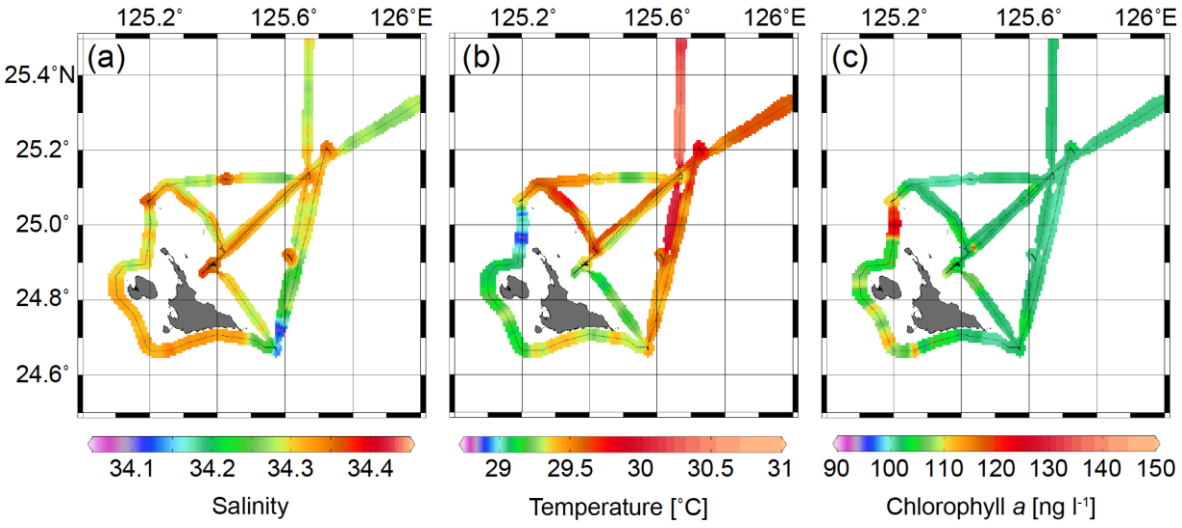

708

709

710 Figure 4. Surface (a) salinity, (b) temperature, and (c) chlorophyll *a* during the

711 KT-09-17 cruise.

712

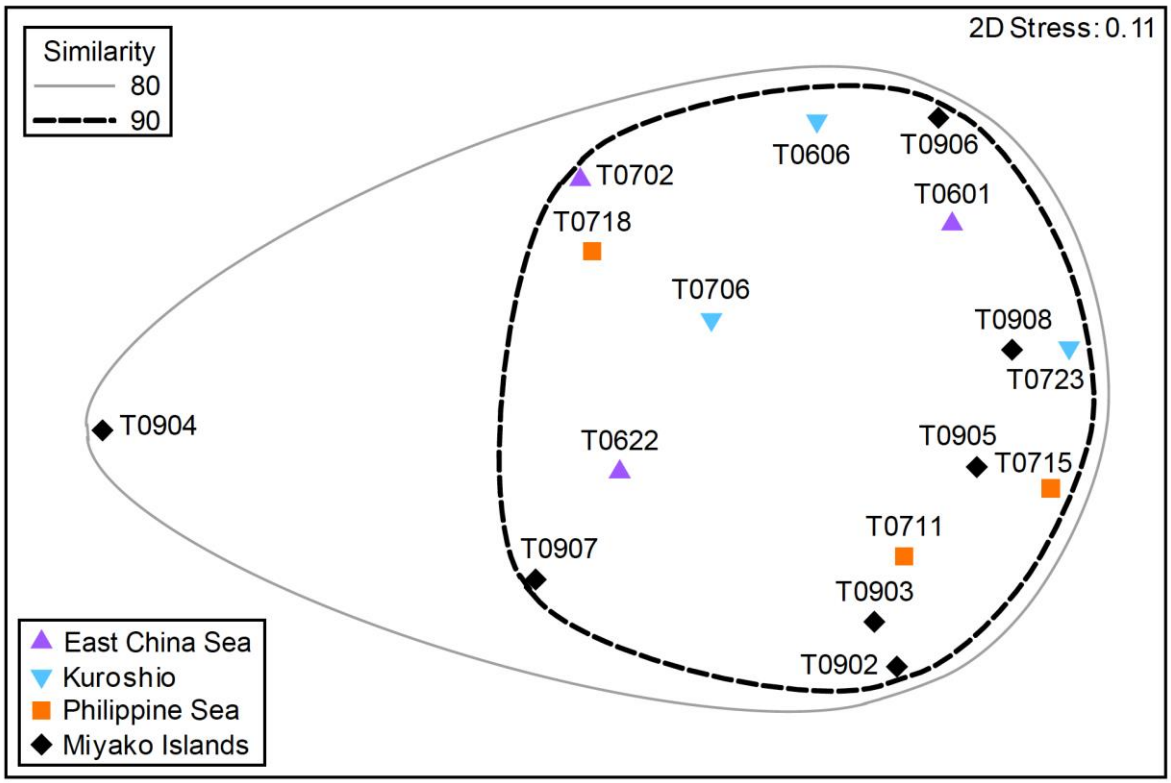

713

714

715 Figure 5. nMDS ordination of sampling stations with environmental variables

716

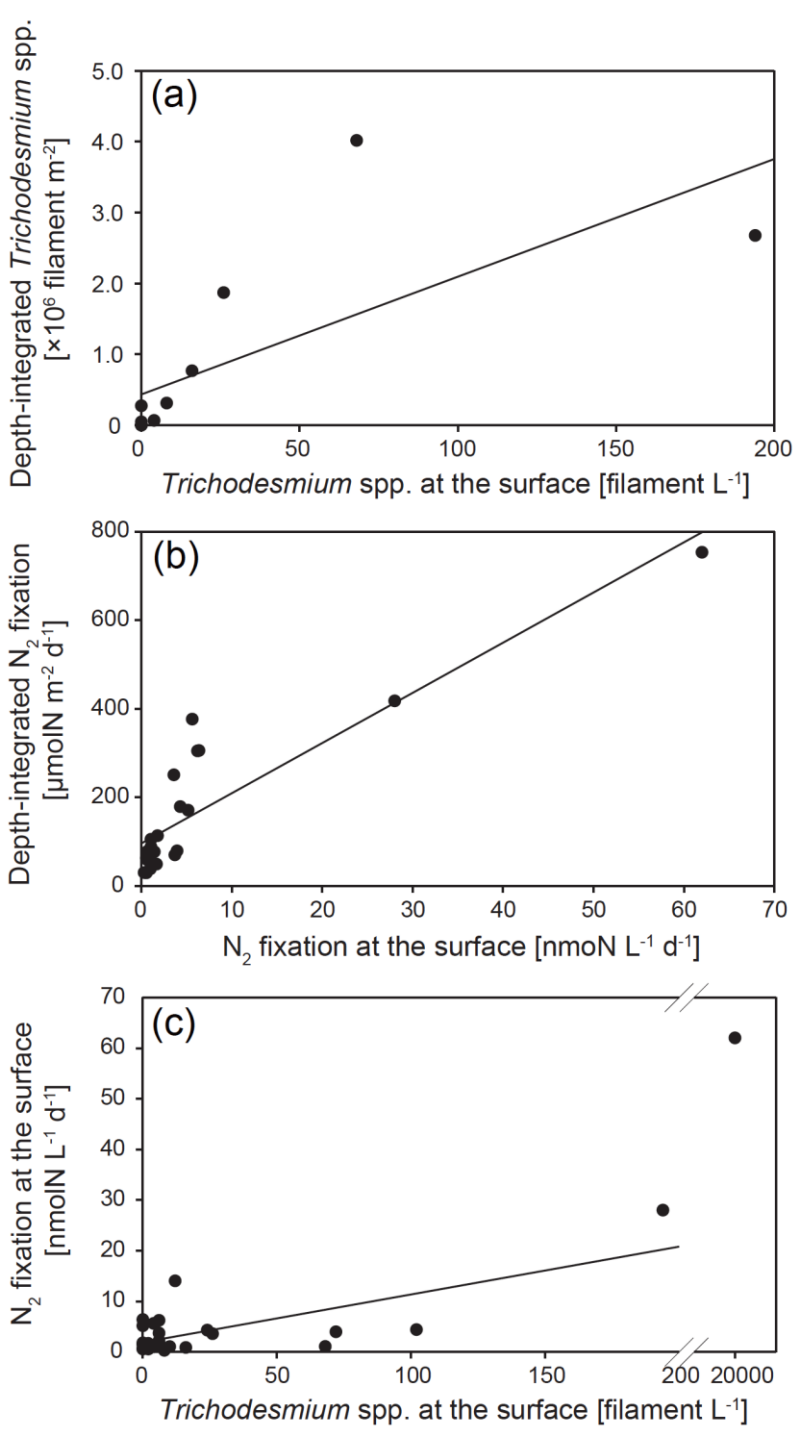
(a)
Depth-integrated Trichodesmium spp. [×10⁶ filament m⁻²]
Trichodesmium spp. at the surface [filament L⁻¹]
(b)
Depth-integrated N2 fixation [µmolN m⁻² d⁻¹]
N2 fixation at the surface [nmoN L⁻¹ d⁻¹]
(c)
N2 fixation at the surface [nmolN L⁻¹ d⁻¹]
Trichodesmium spp. at the surface [filament L⁻¹]

717

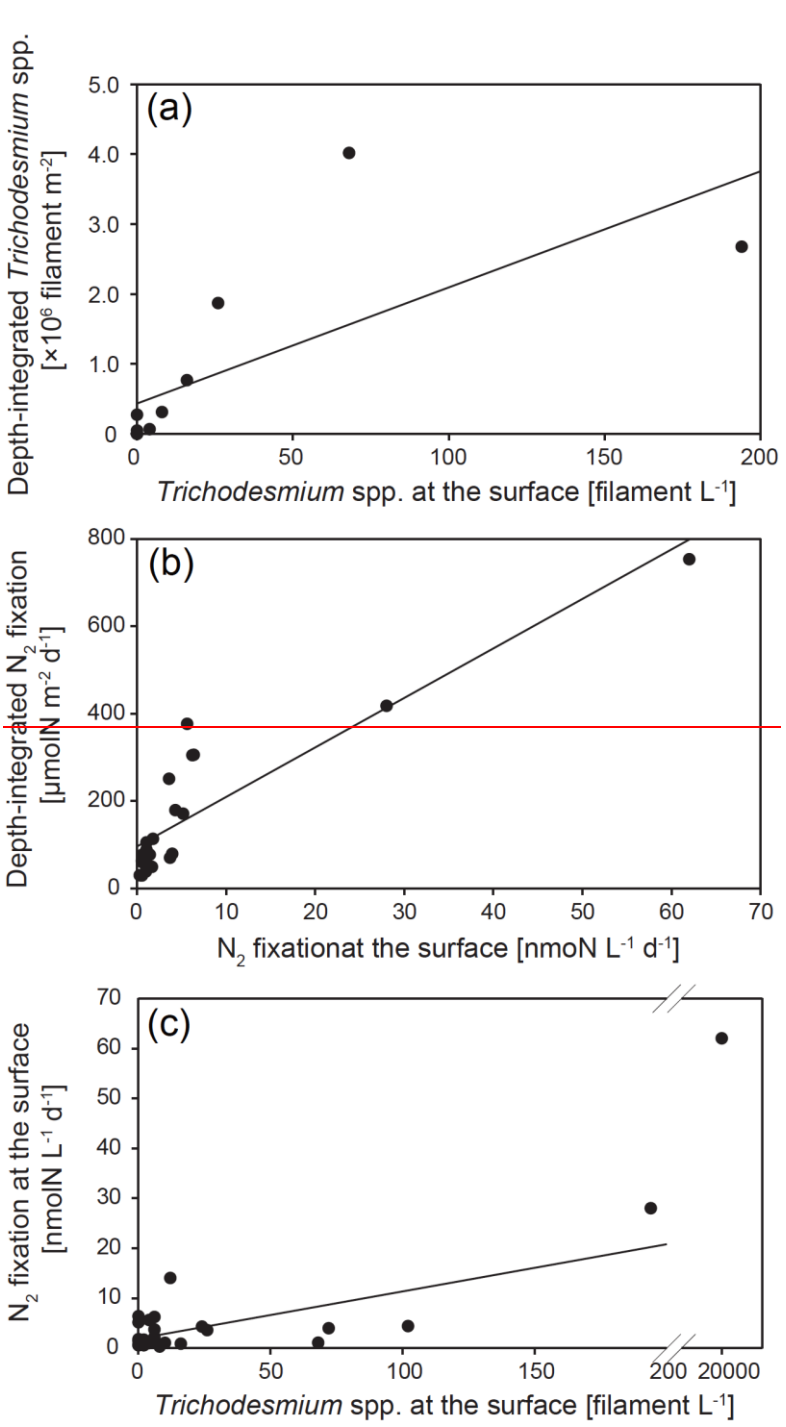

Figure 6. Relationships (a) between surface and depth-integrated *Trichodesmium* spp. abundance, (b) between surface and depth-integrated nitrogen fixation rates, and (c) between *Trichodesmium* spp. abundance and nitrogen fixation rate at the surface.

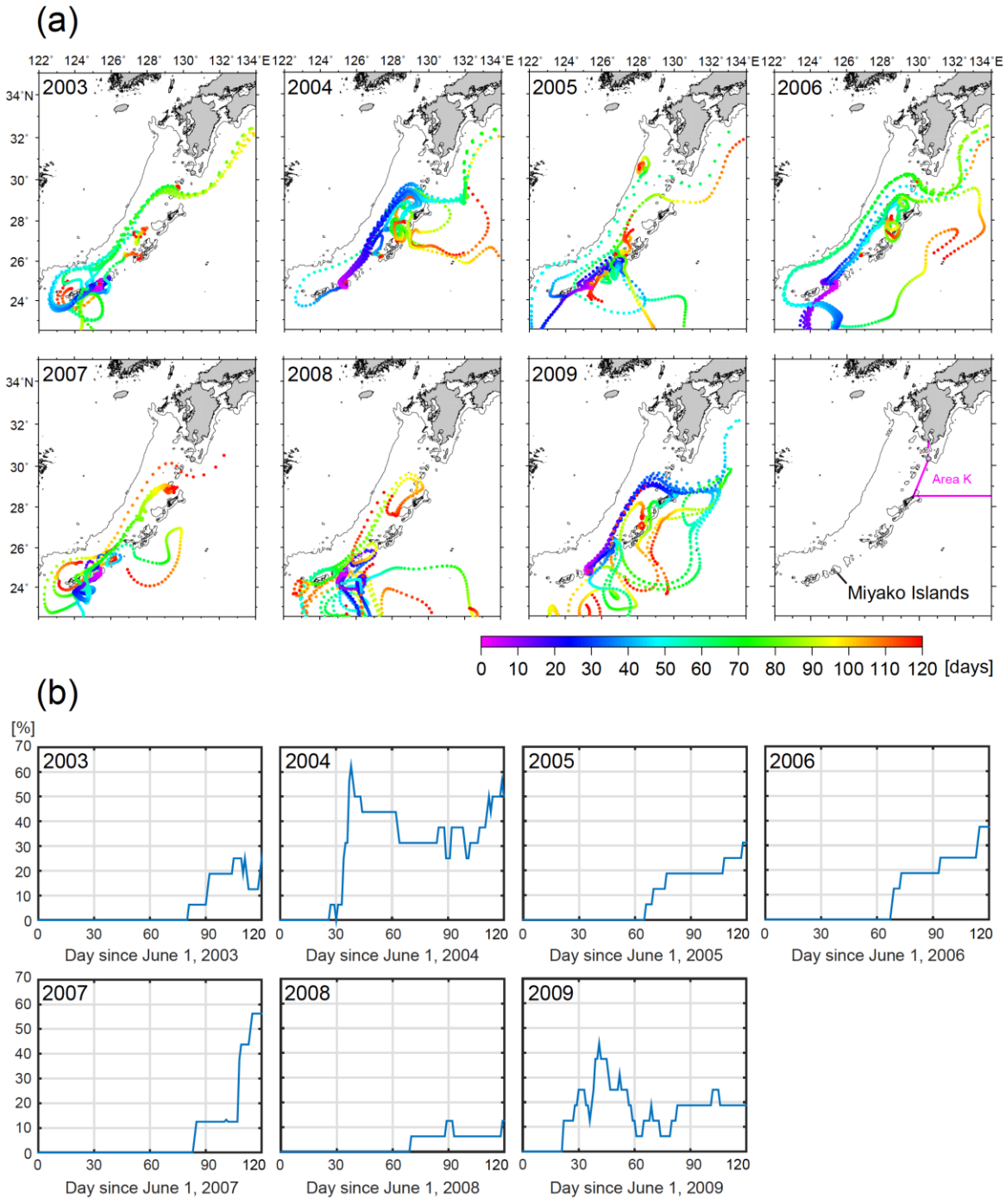

Figure 7. (a) Trajectories of particles released from points around the Miyako Islands on June 1, 2003–2009. (b) The ratio of particles delivered to Area K to the total released particles.